Green Chemistry

PAPER

View Article Online
View Journal | View Issue

Check for updates

Cite this: *Green Chem.*, 2018, **20**, 5196

10 kg scaled-up preparation of Al/Fe-pillared clay CWPO catalysts from concentrated precursors†

Helir-Joseph Muñoz, [a] Carlos Vallejo, [a] Carolina Blanco, [b] Antonio Gil, [c] Miguel-Ángel Vicente, [d] José-Herney Ramírez [e] and Luis-Alejandro Galeano *[a]

In this work, the significant intensification of a bentonite pillaring process was achieved by using a novel methodological approach, leading to an intercalating Al/Fe mixed oligomeric precursor, around 100 times more concentrated than usually reported. In addition, the intercalating step was achieved directly on the clay with no previous swelling of the mineral being required; this allowed the successful scaled-up preparation of the Al/Fe-PILC, by a factor of one thousand, from the lab (10 g) to the pilot scale (10 kg). Intercalating solutions prepared under either concentrated (13 cm^3) or diluted (widely reported, 2.0 dm^3) conditions for lab-scale preparations were both translucent, displaying similar final pH values (close to 4.0) typical of highly oligomerized Al-pillaring solutions. The clay modified from concentrated precursors at the 10 g scale reached a high basal spacing (18.3 Å) and specific surface area (198 $m^2\ g^{-1}$) with very comparable fractions of Fe forming truly mixed Al/Fe pillars in comparison to a reference material (H_2-TPR analyses). This promoted high performance in the catalytic wet peroxide oxidation of phenol in aqueous solution as a toxic model organic molecule at very mild temperature (25.0 °C ± 1.0 °C) and pressure (76 kPa), exhibiting the highest catalytic efficiency as a function of both parameters (full conversion of phenol together with 45.2% of TOC mineralization) with low iron leaching using a very low catalyst concentration (0.25 g dm^{-3}). Particle size refining of the starting clay, the speed of stirring and conditions for the final washing of the interlayered precursor are the main factors influencing successful pillaring at scales higher than 1.0 kg.

Received 3rd August 2018,
Accepted 26th September 2018

DOI: 10.1039/c8gc02445f

rsc.li/greenchem

Published on 24 October 2018. Downloaded by Fail Open on 5/7/2025 8:39:25 AM.

Introduction

A cost-effective and environmentally-friendly change of scale in the production of a solid catalyst from the laboratory (few grams) to pilot-scale (at least several kilograms) require the consideration of numerous factors that may influence the new conditions of production: (i) the avoidance of useless reagents, preparation procedures or solvents; (ii) decreasing the cost of the process as much as possible; (iii) the availability of raw materials; (iv) minimum mandatory purity of chemical reagents; (v) useful final catalyst lifetime; (vi) mechanical, thermal and, especially in the case of Al/Fe-PILCs, chemical stability of the pillaring metals; (vii) resistance to poisoning under reaction conditions, among other aspects.[1,2] The development of cost-effective, high-performing and stable solid catalysts useful at the industrial scale should include prior optimization of the synthesis conditions.[2,3]

The pillaring of clays with Al/Fe confers valuable properties to these materials, since it allows the opening of the clay sheets to basal spacing values in the range of 15.0 to 20.0 Å, mainly by means of the interlayering of Keggin-like Al/Fe-polyoxocations with statistical diameters close to 8.8 Å.[4,5] Once this is achieved, the modified materials display much higher specific surface area and porosity, mainly represented by new micropore content, improved chemical and thermal stabilities, as well as greater access to the active sites stabilized in the interlayer space.[6–8] However, the standard procedure for the lab-scale preparation of pillared clays must allow efficient

[a]*Grupo de Investigación en Materiales Funcionales y Catálisis (GIMFC), Departamento de Química, Universidad de Nariño, Calle 18, Cra. 50 Campus Torobajo, 520002 Pasto, Colombia. E-mail: alejandrogaleano@udenar.edu.co, hjmunoza@unal.edu.co, carlosvallejo@udenar.edu.co*

[b]*Departamento de Química, Universidad Nacional de Colombia, Ciudad Universitaria, Cra. 30 # 45-03, 111321 Bogotá, Colombia. E-mail: cblancoj@unal.edu.co*

[c]*INAMAT-Departamento de Química Aplicada, Edificio de los Acebos, Universidad Pública de Navarra, Campus Arrosadia, 31006 Pamplona, Spain. E-mail: andoni@unavarra.es*

[d]*Departamento de Química Inorgánica, Facultad de Ciencias Químicas, Universidad de Salamanca, Plaza de la Merced, s/n, 37008 Salamanca, Spain. E-mail: mavicente@usal.es*

[e]*Grupo de Investigación en Materiales, Catálisis y Medio Ambiente, Departamento de Ingeniería Química y Ambiental, Facultad de Ingeniería, Universidad Nacional de Colombia, Ciudad Universitaria, Cra. 30 # 45-03, 111321 Bogotá, Colombia. E-mail: jhramirezfra@unal.edu.co*

† Electronic supplementary information (ESI) available. See DOI: 10.1039/c8gc02445f

This journal is © The Royal Society of Chemistry 2018

Published on 24 October 2018. Downloaded by Fail Open on 5/7/2025 8:39:25 AM.

cation exchange as well as high uniformity in the spatial distribution of the interlayered species, with no gelling of the clay throughout the process, which usually represents a big challenge. Such a procedure requires long preparation times and large operating volumes of water (approximately 3.2 dm^3 per gram of final pillared clay) to dissolve metal precursors, disperse the starting clay mineral and to avoid an excess of non-specifically adsorbed (non-interlayered) metal ions on the surface of the clay.[5] Such a set of preparation conditions represent a clear disadvantage from the environmental and economic point of view, which has seriously prevented the preparation of pillared clays at the pilot and industrial scales. As far as we know, the maximum amount of Al/Fe-PILC catalyst that has been reported per single preparation is around 1.0 kg, starting from diluted precursors and using large amounts of water as solvent.[9]

The standard method for the preparation of PILCs at the laboratory scale by hydrolysis with dissolved bases has been extensively studied, yielding intercalating solutions (containing single Al or mixed Al/(transition metal)-oligomers) displaying low Total Metal Concentration (usually TMC < 0.1 mol dm^{-3}).[5,7,10,11] Afterwards, the intercalating step itself is also often performed on highly diluted dispersions of the clay in water (~2.0–5.0% w/v). Accordingly, along the past two decades, a key challenge in the field of the Al/Fe-pillared clays has been to achieve its scaled-up preparation from concentrated precursors while preserving most of their physicochemical features and catalytic response. We recently achieved the preparation of Al/Fe pillared clays[12] using more concentrated precursors (TMC ≈ 0.63 mol dm^{-3}; hydrolysis ratio (OH/(Al + Fe) = 1.6); it allowed the decreased volume of the clay dispersion by around ten-fold, as compared to that widely reported in diluted conditions.[5,7] Other studies have focused on the reduction of the preparation time, involving the use of either microwaves[13] or ultrasound[14] in the step of preparation of the metal intercalating precursor. Moreover, such technologies are energy-intensive, making them not very attractive for preparations at the industrial level.

On the other hand, some researchers[15,16] have reported the straightforward addition of raw clays (not previously swollen) to intercalating Al or Al/Fe solutions, attaining Al- or Al/Fe-pillared materials with basal spacing around 18 Å, a significant increase in specific surface area and pore volume, as well as high-performance in several catalytic applications such as the hydroisomerization of *n*-heptane or the catalytic wet peroxide oxidation (CWPO) of organics dissolved in water. Other researchers have focused on overcoming the aforementioned technological disadvantages of the process by studying pillaring from either concentrated dispersions and/or concentrated hydrolyzed metal solutions.[5] However, as far as we know, currently there are no full solutions to these issues and general reports about the application of this type of clay catalysts at the industrial level are not yet available.

The Al/Fe-PILC clay catalysts have been extensively studied for the degradation of several organic pollutants in water, including dyes,[10,17,18] emerging pollutants,[19,20] phenolic compounds[7,21] and natural organic matter,[12,17] among others. Some recent reports at the laboratory level[7,22,23] have revealed the good catalytic performance of Al/Fe pillared clays in the CWPO degradation of phenol in dilute aqueous systems. Phenol is a frequently investigated contaminant in wastewaters (*e.g.* chemical, petrochemical and agro-food industries) mainly due to its high toxicity, bioaccumulation, poor biodegradability and carcinogenicity,[24,25] as well as environmental concern. This is why it is a useful toxic model organic molecule for improving the preparation of this very promising type of catalyst, which might allow high and cost-effective mineralization of this kind of contaminants at the plant scale in the short term.

Accordingly, this work has been devoted to reporting for the first time the successful preparation of the Al/Fe-PILC clay catalysts from concentrated precursors at the 10.0 kg pilot-scale. The physicochemical and catalytic properties of the resulting material were compared with those displayed by solids prepared at the 10.0 g lab-scale (from either diluted or concentrated precursors) and 1.5 kg bench-scale (from concentrated precursors), both as reference preparations. The catalytic performance of the obtained materials was assessed in the CWPO degradation of phenol at 25 °C and pH = 3.7.

Experimental section

Materials

The starting material used in the preparation of the clay catalysts was a natural bentonite from Cauca Valley, Colombia, called Class 2, which was subjected to two different refining procedures. The first refining method carried out independently (denoted r or R) involved the separation of the fraction from the starting mineral with particle size ≤2 μm. These fractions were mainly composed of smectite phases[26] and they were employed for the two lab-scale (15 g (r) and 10 g (R)) as well as the 1.5 kg bench-scale (R) preparations. The chemical composition of the refined material (r) was (% w/w): 60.44% SiO_2, 21.87% Al_2O_3, 11.04% Fe_2O_3, 0.04% MnO, 2.75% MgO, 1.05% CaO, 0.54% Na_2O, 0.93% K_2O and its cationic exchange capacity (CEC) was 192 meq per 100 g (dry-basis), whereas for the R refined material, it was 56.14% SiO_2, 22.15% Al_2O_3, 10.13% Fe_2O_3, 1.15% TiO_2, 2.95% MgO, 1.53% CaO, 0.88% K_2O and 149 meq per 100 g. Another refining method (denoted RI) was a simpler industrial-like procedure consisting of the drying of the starting mineral in a rotary kiln, followed by grinding to 200 mesh in a Reynolds mill. This method was previously applied to the solid used in the 10.0 kg pilot-scale experiment. The chemical composition of RI material was (% w/w): 52.27% SiO_2, 25.97% Al_2O_3, 13.54% Fe_2O_3, 1.47% TiO_2, 2.34% MgO, 1.06% CaO, 1.52% Na_2O, 0.33% K_2O, and its CEC = 152 meq per 100 g (dry basis).

The pillaring concentrated solutions (prepared separately for each scale) were prepared from $AlCl_3{\cdot}6H_2O$ (97%, Merck®), $FeCl_3{\cdot}6H_2O$ (97%, Panreac®) and elemental aluminum (99.9%, Panreac®), which were all used as received. The diluted pillar-

Published on 24 October 2018. Downloaded by Fail Open on 5/7/2025 8:39:25 AM.

ing solution was prepared from the same reagents but using NaOH (99.0%, Merck®) instead of elemental aluminum. Catalytic experiments were conducted, employing phenol (99.0%, Sigma–Aldrich®) and hydrogen peroxide (50% w/w, Chemí®) used as received too.

Preparation of the Al/Fe – pillared materials

Lab and bench-scale preparations. Preparations of the pillared clays from concentrated precursors at the 10.0 g scale (denoted R-LC; for a detailed explanation of the notation of solutions and solids, please check Tables 1 and 2) were carried out by adapting the method based on the dissolution of elemental aluminum,[15] not previously reported for mixed Al/Fe-solutions. Solutions with nominal TMC value (Al^{3+} + Fe^{3+}) of 5.0 mol dm^{-3}, atomic metal ratio of Fe (AMR_{Fe}) = 5.0% and starting (Al^{3+}/Al^{0}) atomic ratio = (14/86) were prepared for the lab and bench scales (denoted LC and BC, respectively) by mixing $AlCl_3{\cdot}6H_2O$ and $FeCl_3{\cdot}6H_2O$ in the lowest possible volume of water, followed by the slow addition of powdered elemental aluminum at 70 °C under gentle stirring and reflux until full dissolution. The resulting concentrated solution was then aged under constant stirring at 70 °C for around 5.5 h and left to stand at room temperature for a further 38 h. Afterwards, the lab-refined R clay was slowly added over 4 h under constant, gentle stirring at 70 °C to the previously prepared Al/Fe-hydrolyzed concentrated precursor in the correct amount to obtain a final loading of 20 meq (Al^{3+} + Fe^{3+}) g^{-1} clay,[12] according to the method reported elsewhere.[15,16] Thereafter, the resulting concentrated clay dispersion was kept at 70 °C for 8 h under vigorous stirring and finally left to stand for 12 h at room temperature. The solids were then washed with type 2 water using dialysis tubing cellulose membrane (average flat width 43 mm, Sigma®); in this method, the clay dispersion was introduced into the dialysis membrane that was in turn immersed in a 2 L glass beaker containing type 2 water (~80 cm^3 type 2 water per g clay). The water in the beaker was changed periodically until the conductivity dropped to around 20 μS cm^{-1} in the washing liquors. The washed material was then dried at 60 °C (intermediates denoted R-LiC and R-BiC, "i" denoting interlayered), and finally heated in air at 400 °C for 2 h.

The reference Al/Fe-PILC catalyst from diluted precursors at the lab-scale (10.0 g denoted r-LD, see Table 2) was prepared by the standard method of hydrolysis using NaOH solution that was dropped very slowly, as widely reported for the Al/Fe-system.[5,7,10,11] In this case, the pillaring solution (LD) was

Table 1 Physicochemical properties and stirring speed used in the preparation of intercalating solutions, and the amount of clay modified under either diluted or concentrated conditions

Intercalating solution	TMC_f [a] (mol dm^{-3})	pH	Density (g cm^{-3})	Total volume prepared (dm^3)	Stirring speed (rpm)	Amount of clay modified (g)
LD	0.05	4.60	1.01	1.965	>1000	15.0
LC	2.70	4.12	1.15	0.013	>1000	10.0
BC	5.73	3.30	1.33	2.000	<400	1.5×10^3
PC	3.89	3.63	1.30	18.000	<400	1×10^4

[a] Final total metal concentration, experimentally determined. LD: Intercalating solution prepared at the lab-scale under diluted conditions. LC: Intercalating solution prepared at the lab-scale under concentrated conditions. BC: Intercalating solution prepared at the bench-scale under concentrated conditions. PC: Intercalating solution prepared at the pilot-scale under concentrated conditions.

Table 2 Al_2O_3 and Fe_2O_3 contents normalized to the SiO_2 in the starting material, cationic exchange capacities, compensation of CEC, basal spacing and textural properties of starting and pillared clays

Sample	Content[a] (w/w%)		$Fe_{incorporated}$ (Fe_2O_3 wt%)	CEC[b] (meq per 100 g)	CC[c] (%)	d_{001} [d] (Å)	S_{BET} (m^2 g^{-1})	S_{Ext} (m^2 g^{-1})	$V_{\mu p}$ (cm^3 g^{-1})
	Al_2O_3	Fe_2O_3							
r	19.88	14.43	NA	192	NA	15.0	105	50	0.016
R	20.33	11.93	NA	149	NA	14.0	60	45	0.006
RI	24.48	13.90	NA	152	NA	15.9	96	69	0.012
r-LD	27.02	17.83	3.39	78	59	17.4	194	32	0.063
R-LC	31.19	13.79	1.86	35	76	18.3	198	29	0.066
R-BC	28.98	15.76	3.83	115	29	17.7	170	45	0.050
RI-PC	35.34	17.65	3.75	107	30	17.1	147	51	0.039

[a] X-ray fluorescence measurements. [b] CEC (%) = cation exchange capacity (dry-basis). [c] CC (%) = percentage of the cationic exchange capacity of the starting material that was compensated by the intercalating solution. [d] Obtained from powdered samples. NA = not applicable for this sample. r: Refined clay at the lab scale (50 g) by separation of the fraction with particle size ≤2 μm. R: Refined clay at the bench scale (2.0 kg) by separation of the fraction with particle size ≤2 μm. RI: Refined clay at the pilot scale (10.0 kg) through an industrial-like, simpler procedure. r-LD: Refined clay at the lab scale (r) modified at lab-scale (L) from a diluted precursor (D). R-LC: Refined clay at the bench scale (R) modified at lab-scale (L) from a concentrated precursor (C). R-BC: Refined clay at bench scale (R) modified at bench-scale (B) from a concentrated precursor (C). RI-PC: Refined clay at the industrial scale (RI) modified at the pilot-scale (P) from a concentrated precursor (C).

 This journal is © The Royal Society of Chemistry 2018

Published on 24 October 2018. Downloaded by Fail Open on 5/7/2025 8:39:25 AM.

adjusted to the targeted final TMC of 0.06 mol dm^{-3}, AMR_{Fe} value of 5.0% and molar hydrolysis ratio (OH/(Al + Fe)) = 2.4. Afterwards, the diluted pillaring solution was added dropwise to the required amount of 2.0% (w/v) dispersion of the refined powdered clay (r) in water to accomplish 20 meq (Al^{3+} + Fe^{3+}) g^{-1} clay. The obtained interlayered clay (denoted r-LiD) was repeatedly washed with type 2 water (dialysis membrane), dried at 60 °C and calcined at 500 °C for 2 h.

Pilot-scale preparation. The preparation of the intercalating concentrated solution, as well as the step of clay-intercalation, were both performed in the assembly illustrated in Fig. 1: (1) a 304-stainless steel reactor with maximum operational volume of 80 dm^3, electronic-controlled mechanical stirrer (up to 320 rpm) with two Rushton impellers and another impeller at the end of the stirring axis powered by a 1.0 HP engine. The employed stirring axial flow rate ensured the complete mixture of the fluids and dispersed solids inside the reactor (down-up pattern), avoiding gradients of concentration or temperature; in addition, four baffle plates adhered to the inner walls of the reactor improved the hydrodynamic properties such as the turbulence, allowing a greater homogenization of the mixture; (2) a 304-stainless steel condenser in order to prevent the vaporization of the solvent or dispersion medium; (3) a fan made of iron and aluminum to prevent the accumulation of the hydrogen generated after the addition of elemental aluminum; (4) a 304-stainless steel hydrogen burner to safely eliminate hydrogen; (5) a thermostatic bath (Lauda Alpha® RA 12) linked to a 304-stainless steel spiral heat exchanger for temperature control; (6) polyethylene 250 dm^3 storage tank; (7) 0.8 HP centrifuge pump (Pearl®) that allowed movement of the solution/clay dispersion between the reactor and the storage tank; and (8) a doser of solids connected to an air compressor (2.0 HP), which injected previously filtered pulses of air, thus facilitating the slow addition of the solid particles to the bottom of the reactor throughout the stepwise addition of powdered elemental aluminum and the later intercalation of the clay mineral by slow addition of the starting mineral RI.

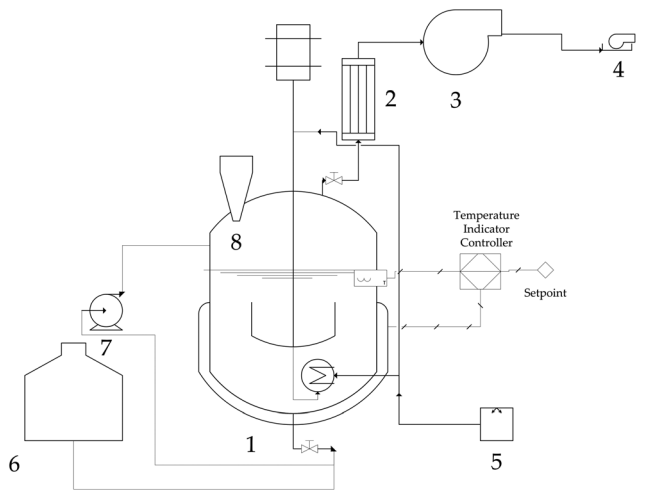

Fig. 1 Preparation scheme of the Al/Fe-pillared clay at the 10.0 kg scale: (1) reactor; (2) condenser; (3) fan; (4) hydrogen burner; (5) thermostatic bath; (6) storage tank; (7) centrifuge pump; (8) solid doser.

The intercalation of the Al/Fe-pillared clay at the 10.0 kg scale (denoted RI-PC, Table 2) was carried out by using around 18.0 dm^3 of the concentrated intercalating precursor (IPC) prepared by the *in situ* use of elemental aluminum as explained before and the accurate amount to modify the starting mineral under identical targeted conditions of TMC, AMR_{Fe}, (Al^{3+}/Al^0) and the Al/Fe-pillar density. However, in this case, the dissolution of the elemental aluminum took a longer time (2 h) than at either the lab- or bench-scale, followed by thermal aging under stirring at 70 °C for around 5.5 h. Thereafter, it was left to stand at room temperature for 38 h before the addition of the pilot-like refined powdered clay (RI) through 4 h at 70 °C under 320 rpm stirring; the dispersion of the Al/Fe-interlayered (RI-PiC) clay was then left to stand at room temperature overnight. The dispersed solid product was then washed several times by recirculation between the reactor and the storage tank, as follows: in the reactor, the interlayered clay was washed with around 15 dm^3 of tap water pumped through a hosepipe under continuous stirring; in the storage tank the washed clay-dispersion was settled-down for 4 h every cycle. This cycle was repeated several times until the conductivity of the washing effluents was around 100 μS cm^{-1} (removed by a 0.5 HP pump). The final interlayered clay was dried at 60 °C and finally heated at 400 °C/air for 2 h, using a heating rate of 10 °C min^{-1}.

Analytical methods

The elemental analyses for Al and Fe content were made *via* atomic absorption spectroscopy (AAS) using a PerkinElmer 2380 apparatus, on samples of around 50 mg that were previously digested in a 4.0 cm^3 : 1.0 cm^3 mixture of HF (40% v/v, Panreac®)/HNO_3 (65% v/v, JT Baker®) per 10 mg of dry solid sample (refined starting minerals and pillared clays from concentrated and diluted precursors). Chemical compositions for the refined starting minerals (R and RI) were also carried out by X-ray Fluorescence (XRF) in a Bruker S8 TIGER equipment of 4 kW dispersive wavelength, with a Rh anode as the source of X-rays and scintillation (heavy elements, from Ti to U) and flow (light elements, from Na to Sc) detectors. The CEC of the materials was determined by the saturation of every solid under reflux with 2.0 mol dm^{-3} of ammonium acetate solution (97%, Carlo Erba®), 45 cm^3 solution per g solid, followed by several cycles of washing with type 2 water and centrifugation to remove excess ammonium ions. The content of exchanged NH_4^+ was then determined by micro-Kjeldahl analysis and expressed as (meq NH_4^+ per 100 g solid).

Powder X-ray diffraction patterns were determined in a Bruker D8 Advance diffractometer at 40 kV and 30 mA under a scanning rate of 2° (2θ) min^{-1}, using filtered CuK_α radiation (λ = 1.5416 Å). The materials were analyzed by default in the range (2–70°2θ). Textural analyses were carried out from the nitrogen adsorption–desorption isotherm at −196 °C, obtained in a Micromeritics 3 Flex Sorptometer in a broad range of relative pressures (around 1 × 10^{-4} mm Hg–1.0 mm Hg) on

Published on 24 October 2018. Downloaded by Fail Open on 5/7/2025 8:39:25 AM.

samples (100–200 mg) previously degassed at 300 °C/12 h. The BET specific surfaces (S_{BET}) were determined by the multipoint BET model using the Keii–Rouquerol criteria to find the proper linear BET range for every sample by means of a procedure based on two principles: (i) the C constant had to be positive and (ii) the application of the BET equation must be limited to the range where the term $V(1 - p/p_0)$ continuously increased with p/p_0.[27] The external surfaces (S_{Ext}), micropore volumes ($V_{\mu p}$) and micropore surface ($S_{\mu p}$) were all calculated from the t-plot (Harkins-Jura de Boer) model. Micropore size distributions were determined from the Horvath and Kawazoe (HK) method, suitable for the predominantly slit-pore morphology featuring pillared clays.[28]

The simultaneous thermal analyses (TGA/DSC) of the interlayered precursors (not still heated at the higher temperature) were recorded in an SDT Q600 TA Instruments apparatus; the measurements were made at a heating rate of 10 °C min^{-1} under a flow of 20 cm^3 min^{-1} of chromatographic zero air gas (mixture 78.1% of N_2 99.999% and 21.9% of O_2 99.6 ± 0.5% of absolute accuracy, Cryogas®) from room temperature to 1000 °C. Hydrogen temperature-programmed reduction analyses (H_2-TPR) were carried out in a Micromeritics Chemisorb 2720 instrument provided with TPx unit controlling temperature rate and ramp; around 150–200 mg of sample was pretreated at 200 °C for 1 h under nitrogen atmosphere and then heated from 250 °C to 1000 °C at 10 °C min^{-1}, under a total flow of 50 cm^3 min^{-1} of reducing gas (10.0% H_2/90.0% Ar). Hydrogen consumption was followed by a thermal conductivity detector (TCD) and Ag_2O (99.99%, Fisher Scientific) was used as an external standard for the calibration of the peak's area.

Catalytic experiments

The catalytic performance of the materials was tested in the CWPO phenol oxidation in a diluted aqueous system. The reactions were carried out at 25 °C (jacketed bath-controlled) and atmospheric pressure (76 kPa) in a 1500 cm^3 glass semi-batch reactor (Pyrex®) equipped with continuous feeding of H_2O_2 solution (Masterflex® peristaltic pump Cole-Parmer), with constant air bubbling, continuous saturation of the liquid phase and removal of the CO_2 produced through the oxidative mineralization of the contaminant and an electronically-controlled mechanical stirrer (LB PRO® OS20-S, 50–2200 rpm). For each test, the reactor was loaded with 0.5 g of catalyst dispersed in 500 cm^3 of 2.8×10^{-4} mol dm^{-3} phenol solution (equivalent to 26.1 mg dm^{-3} of total organic carbon TOC). After the completion of the 30 min of the pre-equilibrium period under constant stirring (600 rpm), 100 cm^3 of 0.0379 mol dm^{-3} H_2O_2 (equivalent to the theoretical stoichiometric amount required for full oxidation) was added under a constant flow rate of 1.67 cm^3 min^{-1} (zero time of reaction). The pH was kept as close as possible to 3.7 throughout the catalytic testing by the manually controlled dropping of either hydrochloric acid or sodium hydroxide 0.1 mol dm^{-3}. The total recorded reaction time, with several sampling periods, was 240 min. The measured response parameters were TOC for the degree of mineralization (Shimadzu TOC-L CPH Analyzer) and spectrophotometric change in the absorbance at λ = 254 nm (UV-2600, Shimadzu) for the indirect recording of the removal of the aromatic content. Phenol conversion was followed by high-performance liquid chromatography (Shimadzu Prominence LC 20) using a C18 column (Luna Phenomenex, 250 mm × 4.6 mm), a PDA detector (fitted to 210 nm and 270 nm) and a mixture of H_3PO_4 solution (pH 2.3)/methanol as the mobile phase (gradient). Before each measurement, each sample was filtered (0.45 μm Millipore) to remove dispersed particles of the catalyst. At the end of every catalytic test, the remaining powdered catalyst was recovered by vacuum filtration and its chemical stability was checked by means of the concentration of leached iron in the reaction's effluent (AAS).

Results and discussion

Physicochemical characterization

The TMC_f (Final Total Metal Concentration) values of the intercalating solutions prepared under concentrated conditions (LC, BC and PC; Table 1) showed that the alternative methodology through the *in situ* dissolution of Al^0 allowed the preparation of stable intercalating precursors (Fig. 2, translucent, free of dispersed particles) displaying final concentrations of metals that were between 54 (2.70 (mol dm^{-3})/0.05 (mol dm^{-3})) and 115 (5.73 (mol dm^{-3})/0.05 (mol dm^{-3})) times more concentrated than the solution prepared under the standard diluted conditions (LD). In addition, LC displayed a final pH value of 4.1, which was within the optimal range for the formation of Keggin-like polyoxocations in diluted systems.[29]

This was indirectly evidenced in the R-LC material using XRD, which showed an interlayer spacing of 8.7 Å (basal spacing 18.3 Å minus layer thickness of 9.6 Å), which is very close to the statistical diameter of the Keggin polycation (~8.8 Å).[4,5] The XRD patterns (Fig. 3) showed that the change from diluted (r-LD) to concentrated medium (R-LC) at the laboratory scale did not affect the expansion of the basal spacing in the intercalating step; furthermore, it was improved to achieve ~1.0 Å greater expansion as compared to r-LD (Table 2). The equivalent hydrolysis ratio (OH^-/(Al + Fe)) for

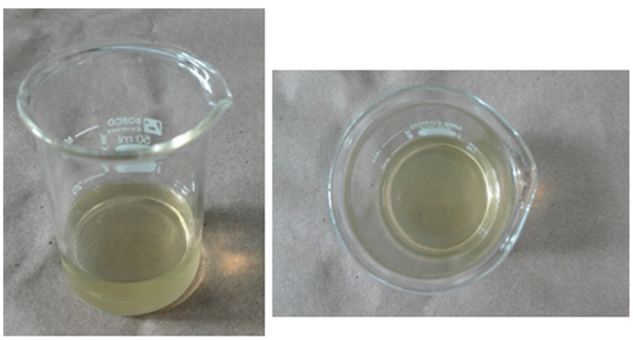

Fig. 2 Intercalating precursor prepared under concentrated conditions at the lab-scale (LC).

 This journal is © The Royal Society of Chemistry 2018

Published on 24 October 2018. Downloaded by Fail Open on 5/7/2025 8:39:25 AM.

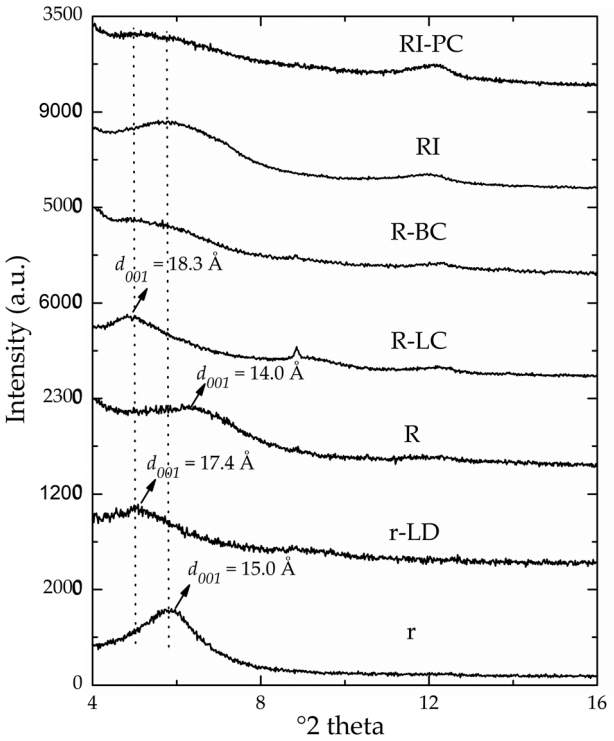

Fig. 3 Low angle region powder X-ray diffraction patterns of starting and Al/Fe-pillared clays.

the solutions prepared under concentrated conditions (LC, BC and PC) was 2.58, a value determined according to the literature procedure,[30] and it was very close to the hydrolysis ratio (HR) value of LD (2.4). This suggested that a high content of the metals condensed to form Keggin-like polyoxocations. Although the CEC in both starting materials (r *vs.* R) differed by around 22% (Table 2), the absolute compensated CEC was almost identical in both corresponding modified materials (r-LD and R-LC) (~113 meq per 100 g, as a result of multiplying the CEC of the starting material by the CC of the modified material), showing that the intercalating power of the concentrated solution (LC) was comparable to that of the diluted one (LD). This was a very important finding since the Al^0 method provides a new preparative route giving access to intercalating solutions that were up to about 80 times (TMC_f = 5.0/0.06) more concentrated than the conventional method, allowing the intensification of the process in one of the most critical stages in the preparation of Al/Fe-pillaring clays, making the scale-up process more feasible. In addition, the pillared R-LC material showed 0.68% CaO, 1.47% K_2O and no content of Na_2O, whereas the pillared material r-LD showed 0.09% CaO, 0.77% K_2O and 0.24% Na_2O, showing that the metal uptake undergone by these materials was mainly carried out *via* the cationic exchange of the starting contents of Ca^{2+} and Na^+ by Keggin-like $(Al/Fe)_{13}^{7+}$-polyoxocations, where K contents could be related to non-swellable phases, probably K-feldspars.[31] Furthermore, hydrogen (H_2) as an evolved by-product through the step of indirect hydrolysis in the preparation of the intercalating precursor could be used in the heating of the same solution; air flow with high energetic potential could be useful for performing such a partial self-heating of the solution.

Both solutions prepared on larger scales (BC and PC) showed pH < 4.0 (Table 1), and there are at least two possible explanations for this. First of all, the low pH values probably indicated that the excess of OH^- ions generated in the aqueous phase by the dissolution of Al^0 reacted very fast to form highly charged and large-sized polymeric species as well as a lower fraction of Keggin-like Al/Fe-polyoxocations.[32] This could be related to the lower stirring speed (less than 400 rpm, in the case of PC), stirrer type (mechanical instead of magnetic) and also due to the higher concentration of metals in both solutions (3.89 mol dm^{-3} *vs.* 5.73 mol dm^{-3}, Table 1), where the final pH may be decreased because of the broader distribution of metal species (in terms of both size and charge).[33,34] In addition, the materials modified with these solutions (R-BC and RI-PC) also showed broader d_{001} signals with fwhm values (full width at half maximum) (Fig. 3) between ~1.30 and ~1.40°(2Θ), which indicated a broader distribution of sizes in the polymeric interlayered species.[35] Secondly, taking into account the similarity in their pH and specifically the low d_{001} values in the materials modified with these solutions (Tables 1 and 2), it is possible that polymeric species were generated with the same degree of hydrolysis but smaller mean size. Thus, it suggests that the self-assembly step to yield the 3D Keggin like polycations was affected in the scaling up, where increasing aging times could be a plausible solution.[32,34] Finally, it was remarkable that the increase in the density of the intercalating solutions (BC and PC) was in agreement with the increases in the final concentrations of metals (TMC_f) (Table 1).

The starting materials with the highest iron contents were RI and r (13.90% w/w and 14.43% w/w, respectively; Table 2). The clay materials may contain a significant content of contaminating phases, possibly as extra-structural iron aggregates. However, the high iron content in RI was probably also caused by contamination during the scaled industrial-like refining process applied to this raw material (detachment of the metal from the mills used), whereas in the r material the Fe could be predominantly located in expansible phases, which favored the purification process. Besides, the elemental analyses (Table 2) showed that all modified materials incorporated Al and Fe irrespective of the intercalating precursor's concentration and the scale (Table 2). The metal uptake was in the range typical of Al/Fe pillared clays prepared at the lab-scale and from diluted precursors, as widely reported.[6,10]

The scale-up in the previous refining clearly worsened the efficiency in the purification of the starting clay. This is probably because the d_{001} signal characteristic of expandable phases was poorly defined in the materials R and RI, in comparison with r material (Fig. 3). However, the most affected physicochemical property as a consequence of the scaling up was the micropore content $V_{\mu p}$ (R = 0.006 $cm^3\ g^{-1}$; RI = 0.012 $cm^3\ g^{-1}$ and r = 0.016 $cm^3\ g^{-1}$); this may be ascribed

Published on 24 October 2018. Downloaded by Fail Open on 5/7/2025 8:39:25 AM.

to the clogging of the micropores by extra-structural iron oxide aggregates.[10] According to Gong *et al.*,[36] an important factor in the loss of yield by purification using a physical method such as that used in our pilot scale extraction could be the grinding time, which should be greater than 75 min in order to obtain particles smaller than 0.5 μm (average diameter ~0.28 μm); apparently, it is essential for the proper dispersion of montmorillonite, which is optimum in the range of 0.1–2.0 μm and average diameter of ~0.5 μm. With this grinding time, bentonite particles were transformed from heterogranular agglomerated to homogenous isometrically dispersed.[36]

The textural properties of the r-LD, R-LC, R-BC and RI-PC materials (Table 2) displayed significantly increased BET surface areas (between 51 $m^2\ g^{-1}$ and 138 $m^2\ g^{-1}$) and micropore volumes (between 0.06 $cm^3\ g^{-1}$ and 0.047 $cm^3\ g^{-1}$) in comparison to their starting materials (r, R and RI, respectively. Table 2); their fractions of external surface in general decreased, although the opposite behavior was observed by increasing the scale of preparation. These characteristics are typical of clays successfully pillared with the binary system Al/Fe.[8,37] The r-LD (S_{BET}: 194 $m^2\ g^{-1}$ and $V_{\mu p}$: 0.063 $cm^3\ g^{-1}$), R-LC (S_{BET}: 198 $m^2\ g^{-1}$ and $V_{\mu p}$: 0.066 $cm^3\ g^{-1}$) and R-BC (S_{BET}: 170 $m^2\ g^{-1}$ and $V_{\mu p}$: 0.050 $cm^3\ g^{-1}$) exhibited approximately three-fold greater specific surface areas and increased between 3 and 11 times their micropore volumes, as compared with their starting materials (r and R); meanwhile, RI-PC (S_{BET}: 147 $m^2\ g^{-1}$ and $V_{\mu p}$: 0.039 $cm^3\ g^{-1}$) only doubled its S_{BET} and its volume of micropores increased by around 3 times in comparison with RI. This means that scaling up to 10 kg mainly affected the textural properties of the final Al/Fe-PILC because the polyoxocationic species formed in the intercalating solution prepared at 18 dm^3 (PC) presented a more heterogeneous distribution of sizes and charges, possibly accompanied by lower intercalating power. Therefore, it generated a lower expansion of the interlayer space as discussed above in the XRD results. In addition, the stirring speed during the intercalation was approximately 1200 rpm lower than at the lab-scale (320 rpm *vs.* 1500 rpm) but approximately the same as at the bench-scale (320 rpm); this may have affected the diffusion efficiency of the cations within the interlayer space of the clay. RI-PC was the only material washed with tap water instead of type II water (equivalent to distilled water), so the extra ions in the washing-water probably competed with the Al/Fe polyoxocations in the interlayer space of the clay. Another factor that affected the final textural properties was the washing method: in the scaled-up preparations a settle-down method was used instead of a dialysis membrane (used at lab and bench scale). The scaled-up washing method probably removed a smaller fraction of adsorbed chloride ions from the interlayered precursor. In fact, the minimum conductivity achieved in the washing-water with the settle-down step method was ~100 μS cm^{-1}; this value was higher than that reached in the final washings with the dialysis membrane method (~20 μS cm^{-1}). In contrast, a positive effect on the intercalated Al/Fe species could be generated using the dialysis membrane, consequently favoring the textural properties of the modified clays (R-LC and R-BC; Table 2), due to changes in the pH and/or ionic strength in the liquid phase generated by this process.[38]

Nitrogen adsorption–desorption isotherms of the starting and pillared materials are presented in Fig. 4. The isotherms of clays modified with the binary system Al/Fe in concentrated and diluted conditions in all scales showed a clear increase in the capacity of adsorption compared to the starting materials, due to the formation of micropores by the effective pillaring as previously discussed. The isotherms of the starting materials were type II according to the IUPAC system,[39] with adsorption related to mesoporous materials.[15] Meanwhile, the isotherms of all the materials modified with the Al/Fe-system were intermediate between type I at low relative pressures (p/p_0) and type II in high p/p_0 according to the BDDT classification,[40] featuring mesoporous and microporous solids.[15] The materials prepared in a concentrated medium at the bench and pilot scales (R-BC and RI-PC) presented adsorption–desorption isotherms with a higher separation between the branches of adsorption and desorption; this means that these materials presented higher capillary condensation,[8] which could be related to broader, heterogeneous distribution of micropore sizes in these clays. In addition, the hysteresis loops were type H3 in the IUPAC classification,[39] typical of slit-shaped pores, indicating that the configuration of parallel plates of clay minerals was fairly preserved.[8,41]

The micropore distributions determined by the Horvath–Kawazoe (HK) method for the starting materials r, R and RI (Fig. 5) showed high heterogeneity in the distribution of pore widths;[28] however, when such materials were pillared with Al/Fe polyoxocations prepared under either diluted (r-LD) or concentrated conditions at different scales (R-LC, R-BC and RI-PC), the heterogeneous distribution of the pore sizes became a well-defined bimodal profile of micropore widths in r-LD, whereas it was accompanied by a little shoulder at the

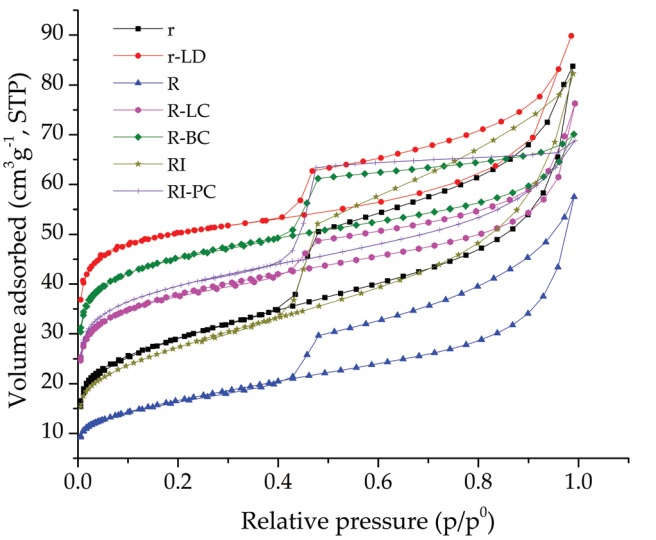

Fig. 4 Nitrogen adsorption–desorption isotherms of starting and Al/Fe-pillared clays.

This journal is © The Royal Society of Chemistry 2018

Published on 24 October 2018. Downloaded by Fail Open on 5/7/2025 8:39:25 AM.

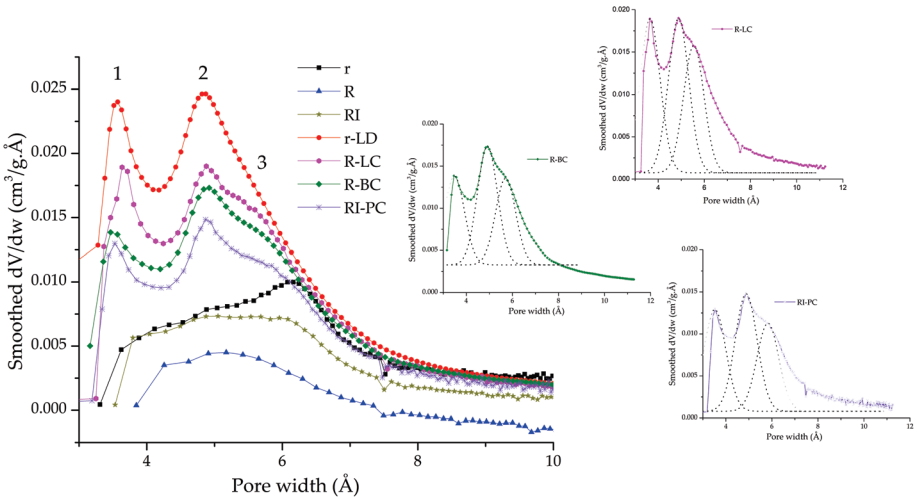

Fig. 5 Micropore size distribution analysis by the Horvath and Kawazoe (HK) method of starting and Al/Fe-pillared clays: solid lines are experimental curves and dotted lines Gaussian fitted curves.

higher pore-width region in the materials modified under concentrated conditions, irrespective of the scale of preparation. Accordingly, it can be safely concluded that effective pillaring of the clays led to the following: (i) average pore widths of ~3.5 Å, which probably corresponded to the intercalation of small oligomeric Al/Fe species with a low degree of hydrolysis; (ii) average pore widths of ~4.9 Å that could be related to Keggin-like mixed Al/Fe oligocations, although they are much lower compared to the statistical diameter in the liquid phase (~8.9 Å), since it is expected to significantly decrease upon heating at high temperature (dehydration and dehydroxylation of Keggin-like polycations, as evidenced by simultaneous thermal analysis of the intercalated materials (r-LiD, R-LiC, R-BiC and RI-PiC, ESI – Fig. S1†). As it can be seen, the interlayered materials showed a mass loss in the range of 304 °C–539 °C, accompanied by an endothermic peak centered at approximately 457 °C.[15] This thermal event occurred at lower temperatures in all the materials modified with the Al/Fe-polycations compared with their starting materials (r, R and RI), due to the presence of the intercalating species. Such a contraction of the observed second pore width maximum in comparison with the Keggin's diameter could also be related to the deviation to lower pore widths than normal, produced by the electrostatic interaction between the quadrupole moment of N_2 and the micropore walls, inducing partial pore blocking and preventing the more accurate evaluation of microporosity, underestimating the true pore width.[5,42,43] (iii) The peak deconvolution in Fig. 5 for materials modified with concentrated precursors showed pore widths centered around 5.8 Å, irrespective of the scale of preparation; this is probably related to interlayered polymeric species, slightly larger than Keggin-like Al/Fe polycations, as discussed above for the XRD results. This suggests that in all intercalating solutions, even in those prepared under diluted conditions, smaller or larger polymeric species than Keggin-like species were also formed.[44] Finally, it can be observed in Fig. 5 that materials prepared from concentrated precursors on all scales (R-LC, R-BC and RI-PC) decreased the intensity of the signal (ii) in comparison to r-LD, apparently because of the increased fraction of polymeric species of smaller ((i) mainly in the case of R-LC) and larger sizes (iii) in their intercalating solutions. In addition, the areas under the curve's deconvolution in the micropore width distributions (Fig. 5) suggested that R-LC showed 2.3 and 1.4 times greater contribution of the smaller polymer species (~3.5 Å) in comparison with R-BC and RI-PC, respectively; it also exhibited 1.3 and 1.2 times more polymeric species of middle average diameter (~4.9 Å) and 1.5 and 1.3 times higher formation of larger polymer species (~5.8 Å) against R-BC and RI-PC, respectively. Thus, although the scaling up in the preparation of the clay catalyst increased the absolute contribution of either poorly or overpolymerized species, the concentration of Keggin-like species also increased by almost the same magnitude, yielding very similar fractions of the micropore's volume as those observed from the lower-scale preparation.

According to SEM analyses, the starting clays (r, R y RI, Fig. 6a, c and f) exhibited aggregates of lamellar particles with a smooth, uniform and flat morphology.[25,45] Images evidenced a noticeable change in the morphology of the functional materials (r-LD, R-LC y R-BC, Fig. 6b, d and e) upon intercalation of the Al/Fe-oxide pillars; it is worth noting that it became very rough and highly porous, in good agreement with the data for specific surface areas (Table 2). The r-LD material yielded flower-like particles, whereas the pillared clays R-LC and R-BC generated structures in tightly-packed patterns; these results are directly related to the intercalation mode employed by Tomul *et al.*[45] They determined that the direct addition of the clay to a Fe/Cr mixed intercalating solution yielded a tightly-packed pattern, while the addition of the intercalating solution to the clay suspension yielded flower-like pores. In the case of RI-PC material, the change in mor-

Published on 24 October 2018. Downloaded by Fail Open on 5/7/2025 8:39:25 AM.

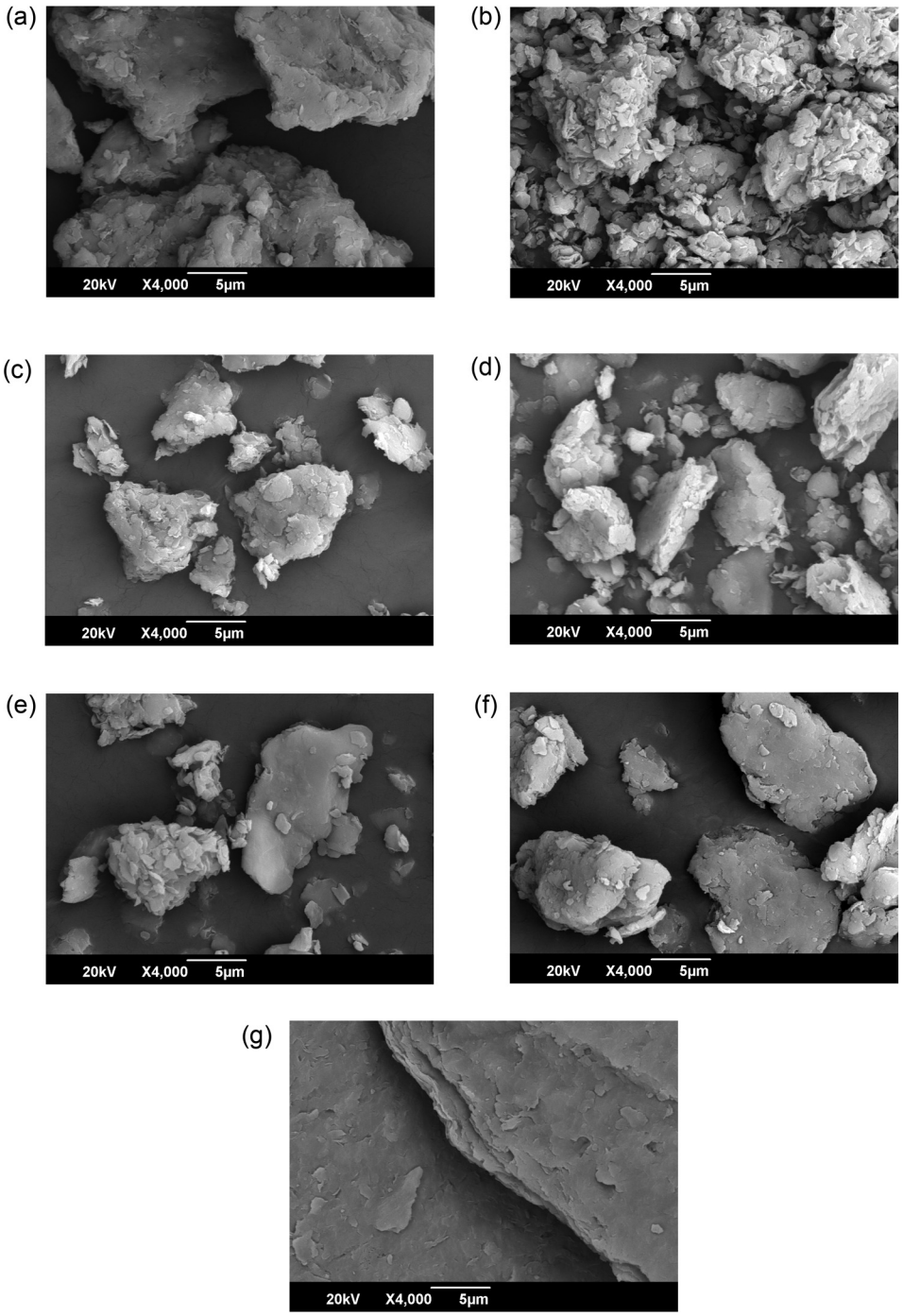

Fig. 6 SEM micrographs (×4000) for Al/Fe-pillared clays: (a) r; (b) r-LD; (c) R; (d) R-LC; (e) R-BC; (f) RI and (g) RI-PC.

phology was not that evident; larger particle sizes were observed, probably because in the purification of the starting material RI by particle size, it only reached a minimum average diameter of ~75 μm (200 mesh).

On the other hand, according to the results of the elemental composition at the surface level as determined by X-ray dispersive energy (EDS) of the modified materials (r-LD, R-LC, R-BC and RI-PC, regions marked in the micrographs of ESI in Fig. S2, S3 and S4† at different magnifications), sodium and calcium were not detected; this was strong evidence of the ion exchange of the Al/Fe-Keggin poly-hydroxycations as the main mechanism of uptake of the metals, supporting what was previously revealed by the XRF analyses. It is remarkable that according to the variance estimated for Fe content for different magnifications in the micrographs (r-LD = 1.16; R-LC = 0.19; R-BC = 0.60 and RI-PC = 4.21), the material with the lowest var-

 This journal is © The Royal Society of Chemistry 2018

Published on 24 October 2018. Downloaded by Fail Open on 5/7/2025 8:39:25 AM.

iance corresponded to the solid prepared at the laboratory scale in concentrated medium (R-LC, 0.19); this value can be used as a criterion for the degree of homogeneity with which the Fe got dispersed on the material's surface, *i.e.*, a higher variance must be expected for samples with higher contributions of large aggregates of Fe oxides. Therefore, it can be inferred that R-LC exhibited the more homogeneous distribution of incorporated active sites, *i.e.*, a greater contribution of Fe isolated species thought to be structurally a part of the mixed pillars stabilized in the interlayer space of the aluminosilicates; it was therefore expected that they would be less detectable by EDS. This material was followed in terms of the same characteristics displayed by R-BC (0.60) and r-LD (1.16) materials; as expected, the RI-PC material displayed an estimated variance higher than 4, suggesting a significantly higher contribution of FeO_x extra-structural aggregates, with relatively high particle sizes.

The H_2-TPR plots (Fig. 7) confirmed that one of the starting materials with the highest Fe contents was RI, which presented higher total consumption of hydrogen in its two most representative reduction events (~305 and 417 μmol H_2 per g, respectively). The two reduction events in all the starting clays can be attributed to (i) the reduction of iron on the external surface (iron contaminating phases), which occurred at lower temperatures between 539 and 588 °C, and (ii) the reduction of the structural iron within the sheets of the clays, which occurs at temperatures between 774 and 846 °C.

However, all materials modified with the Al/Fe-system showed a reduction signal at even higher temperatures, between 900 and 968 °C (just those marked with black squares in Fig. 7), which was not observed in the starting materials and could clearly be attributed to less reducible, true mixed species of Al/Fe (pillars) incorporated into the interlayer space of the clays, as previously proposed.[10]

The decrease in the total consumption of hydrogen displayed by the pillared materials (r-LD, R-LC, R-BC and RI-PC) in comparison with their starting clays (r, R and RI) (Fig. 7) suggested that during the pillaring process a significant fraction of extra-structural Fe aggregates got leached. On the other hand, iron reduced at lower temperatures (500–552 °C) in the expanded materials could be somehow safely ascribed to iron within the structural sheets of the clay, whose reduction might occur at lower temperatures due to greater accessibility granted by the expansion of the clay layers upon Al/Fe-pillaring.

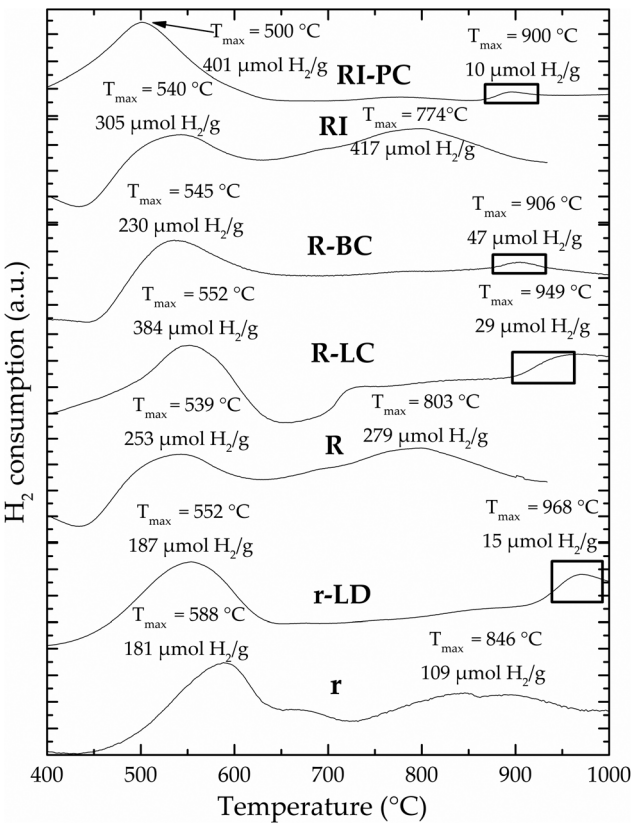

Fig. 7 H_2-TPR diagrams of starting and Al/Fe-pillared clays.

Catalytic performance

The evolution of phenol conversions and TOC mineralizations (%) throughout the CWPO catalytic reaction using the Al/Fe-pillared clays prepared with different concentrations of precursors and scales are compared in Fig. 8. First of all, it can be clearly seen that the change from diluted (r-LD) to concentrated precursors (R-LC) at the lab-scale strongly improved the catalytic performance of the catalyst (Fig. 8a), since R-LC exhibited the highest catalytic efficiency as a function of both parameters (full conversion of phenol and 45.2% of TOC mineralization) at the final time or reaction (including 30 min of pre-equilibrium period) as compared to r-LD, which reached 5.8 mg dm^{-3} of phenol conversion (approximately 23%) and 30.4% of TOC mineralization at very mild conditions of reaction temperature. The best catalytic performance displayed by this catalyst could be specifically related to (i) the higher basal spacing (d_{001} = 18.3 Å) achieved by the effective pillaring of this solid, which allowed greater accessibility of organic substrates and phenol to the active sites, mainly incorporated in the interlayer space of the clay.

Consequently, the increased basal spacing in R-LC led to the following: (ii) higher specific surface area (198 m^2 g^{-1}) mainly by the setting-up of new micropores, wherein the most active catalytic sites could be predominantly located. In addition, this material against r-LD showed (iii) higher hydrogen consumption (29 μmol H_2 per g) in the event of reduction at the highest temperature (949 °C), probably confirming that it is related to the higher abundance of truly mixed Al–Fe pillars, highly active at catalyzing the CWPO reaction. Finally, (iv) the R-LC material presented an elevated absolute compensation of the CEC (113 meq per 100 g), which was pretty similar to that displayed by r-LD; this factor is very important since it reveals a strong correlation between the ability of the polycations to exchange the clay's layer charge and the catalytic performance of the clays upon Al/Fe pillaring in the CWPO

Published on 24 October 2018. Downloaded by Fail Open on 5/7/2025 8:39:25 AM.

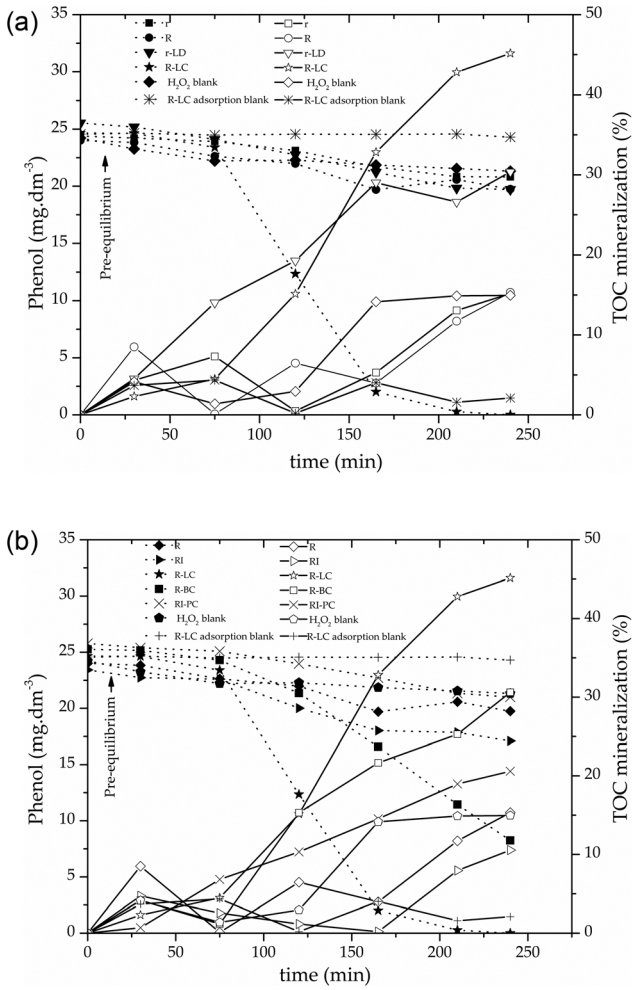

Fig. 8 Catalytic behavior of materials in the CWPO degradation of phenol (dotted lines) and TOC mineralization (solid lines): (a) the effect of the concentration of the intercalating precursor; (b) effect of scaling up in the preparation from laboratory (10 g) to pilot scale (10 kg). Catalyst loading = 1.0 g dm^{-3}; $[Phenol]_0$ = 2.8 × 10^{-4} mol dm^{-3}; $[H_2O_2]_{added}$ = 0.0379 mol dm^{-3}, *V* H_2O_{2added} = 100 cm^3; H_2O_2 stepwise addition = 1.67 cm^3 min^{-1}; pH = 3.7; *T* = 25.0 ± 0.1 °C; ambient pressure = 76 kPa.

reaction.[10] It is noteworthy that the concentration of the active metal (Fe) in the aqueous effluent of the reaction after the catalytic test in the presence of R-LC material was 0.5 mg Fe per dm^3; such a low concentration corresponds to iron leaching below 1.0% of the Fe incorporated in the catalyst, ruling out significant contribution of homogeneous Fenton processes to the recorded catalytic response. Furthermore, it indicates that the active phase was strongly bound to the clay and the pillars, and that the catalyst was highly stable under the strongly oxidizing environment of the CWPO reaction. Meanwhile, the catalyst scaled up to 1.0 kg (R-BC) showed better phenol depletion (approximately 68%) as compared to the r-LD catalyst (approximately 23%), whereas the TOC mineralization in both cases was very comparable (~30%). Taking into account the experimental conditions, probably a reaction time exceeding 240 min is required in both cases to reach 100% phenol conversion. However, when the R-BC and RI-PC catalysts were compared against the R-LC catalyst (Fig. 8b), the catalytic response clearly decreased in both cases, although it was more evident for RI-PC, because it displayed a phenol conversion of 4.7 mg dm^{-3} (approximately 18%) and 20.6% of TOC mineralization. It can be inferred that the catalytic performance of the RI-PC catalyst decreased mainly because of the minor textural properties of this functional material, probably related to the incorporation of polyoxocations having a wider heterogeneous distribution of sizes; this probably limited the internal diffusion of reactants and products of reaction through the catalyst's porosity in the CWPO process. In addition, according to the H_2-TPR analyses (Fig. 7), this material also displayed the lowest content of true mixed Al/Fe-pillars (lower hydrogen consumption corresponding to the signal at about 900 °C: 10 μmol H_2 per g), although it has been reported that low TOC conversion would also be caused by the accumulation of intermediates and by-products, mainly carboxylic acids on the catalyst's surface,[45,46] which inhibit activation of H_2O_2 to hydroxyl radicals, thereby causing the hydroxyl radicals to not be effectively used for the degradation of phenol and its oxidation side products. The blank experiments ruled out simple adsorption (R-LC adsorption blank), significant oxidation by molecular peroxide with no previous catalytic activation (H_2O_2 blank) or significant roles played by the structural iron in the starting clay minerals before the Al/Fe-pillaring modification (r, R and RI) as side phenomena able to explain the recorded phenol depletion and TOC mineralization levels achieved by the Al/Fe-pillared clays. Finally, it must be emphasized that in order to get greater contrast between the studied materials in terms of their catalytic performance, we assessed just tiny concentrations of catalyst together with stoichiometric doses of hydrogen peroxide (no excesses were used, as it is usual in most of the literature reports in the field); thus, the maximal phenol depletion and TOC mineralization displayed by the clay catalysts of course could be further enhanced by the tuning of the following CWPO reaction parameters: catalyst loading, peroxide dose and mode of addition, temperature and pH of the reaction, *etc*.

The by-products of the heterogeneous Fenton reactions require special attention since in many organic substrates some of them could be significantly more toxic than the starting targeted pollutant.[47] In this research, the TOC reduction was in most of the cases lower than the phenol conversion in the presence of all catalysts (Fig. 8a and b), indicating that the oxidation of the contaminant proceeded through the formation of several intermediates before completing mineralization to CO_2 and H_2O.[48] Only oxalic acid was found by liquid chromatography (ESI, Fig. S5a and b†), mainly in the presence of catalysts r-LD and R-LC; it is noteworthy that this is a short chain, non-toxic organic acid,[47] suggesting that a rather easy elimination by microbiological post-treatment could be implemented in the case of wastewaters displaying high CWPO output concentrations of the by-product. Time-evolution curves of oxalic acid (Fig. 9) showed increasing concentration

 This journal is © The Royal Society of Chemistry 2018

Published on 24 October 2018. Downloaded by Fail Open on 5/7/2025 8:39:25 AM.

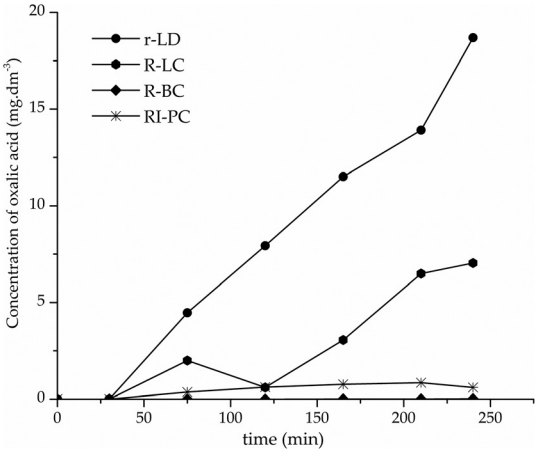

Fig. 9 Time-evolution curves of oxalic acid from CWPO of phenol in the presence of the Al/Fe-pillared clays.

with reaction time, using the aforementioned catalysts. This demonstrates that full mineralization was mainly prevented by the accumulation of oxalic acid at the very final stages of the oxidation pathway, which was the main species recently found to inactivate a Fe^{3+}–Al_2O_3 CWPO catalyst in a continuous flow reactor.[49] Another very interesting aspect displayed by all catalysts was that hydroquinone and *p*-benzoquinone, which are of particular interest due to their higher toxicities against phenol itself,[47] were not identified at all as reaction intermediates (ESI, Fig. S6 and S7†); this means that the full removal of these species is guaranteed by the Al/Fe-PILC activated CWPO reaction, irrespective of the concentration of the precursors or the scale of preparation employed.

Conclusions

A novel, greener methodological approach to the preparation of Al/Fe-PILCs from highly concentrated intercalating metal solutions (up to around 100 times higher than standard) is presented. It produces a stable, particle-free, poly-cationic precursor with an intercalating power pretty close to that displayed by solutions hydrolyzed under dilute conditions (conventional, widely reported procedure). It suggested, in both cases, the almost equivalent formation of Keggin-like $(Al/Fe)_{13}^{7+}$ – mixed polyoxocations, useful for clay expansion, promoting significant intensification of one out of two critical stages involved in the pillaring of clays, making them much more feasible for the scaled-up preparation of Al/Fe-PILCs. Besides, hydrogen (H_2) evolved through the hydrolysis of the intercalating precursor could be used for self-heating of the solution. These clay-catalysts were also successfully prepared by using the concentrated intercalating precursor on starting clay (not previously swollen) at the laboratory scale. The clay modified under such conditions displayed high final basal spacing (18.3 Å), specific surface area (198 $m^2\ g^{-1}$) and a comparable fraction of Fe forming truly mixed Al/Fe pillars, in comparison to reference material prepared from standard, well known diluted precursors. Final physicochemical characteristics promoted high performance in the CWPO of phenol in aqueous medium at a very mild reaction temperature (25.0 °C ± 1.0 °C) and pressure (76 kPa), exhibiting the highest catalytic efficiency as a function of both parameters (complete conversion of phenol and TOC mineralization equivalent to 45.2%) and low iron leaching, ruling out simple homogeneous Fenton degradation. Finally, it was shown that the starting clay's refinement by particle size, stirring and the conditions of the final washing of the interlayered precursors, in this order, are the most influencing factors preventing the successful Al/Fe-pillaring of clays based on Al at scales higher than 1.0 kg from concentrated precursors. The catalytic performance of this kind of material in the CWPO reaction was shown to be very sensitive to the final textural properties, but mainly to the fraction of Fe that could be successfully stabilized in truly mixed Al/Fe-pillars. This novel approach opens an important avenue for several applications of Al/Fe-PILCs at the pilot and industrial scales, mainly within the scope of the environmental catalysis.

Conflicts of interest

There are no conflicts of interest to declare.

Acknowledgements

Financial support received from CT&I Fund of the SGR-Colombia to *CWPO for Enhanced Drinking Water Quality Nariño Project* (BPIN 2014000100020) is kindly appreciated. HJ Muñoz also gratefully thanks MSc. scholarship granted from program "Strengthening of regional capacities in research, technological development and innovation in Nariño Department", call 03/2015, Nariño Department – CEIBA Foundation, Colombia.

Notes and references

1 M. Campanati, G. Fornasari and A. Vaccari, *Catal. Today*, 2003, **77**, 299–314.
2 M. G. Warawdekar, in *Industrial Catalytic Processes for Fine and Specialty Chemicals*, Elsevier, 2016, pp. 721–736.
3 F. Piccinno, R. Hischier, S. Seeger and C. Som, *J. Cleaner Prod.*, 2016, **135**, 1085–1097.
4 J. Zhu, K. Wen, P. Zhang, Y. Wang, L. Ma, Y. Xi, R. Zhu, H. Liu and H. He, *Microporous Mesoporous Mater.*, 2017, **242**, 256–263.
5 M. A. Vicente, A. Gil and F. Bergaya, in *Developments in Clay Science*, ed. F. Bergaya and G. Lagaly, Elsevier, Amsterdam, The Netherlands, 2nd edn, 2013, vol. 5, pp. 523–557.
6 W. Najjar, S. Azabou, S. Sayadi and A. Ghorbel, *Appl. Catal., B*, 2007, **74**, 11–18.

Published on 24 October 2018. Downloaded by Fail Open on 5/7/2025 8:39:25 AM.

7 C. Catrinescu, D. Arsene and C. Teodosiu, *Appl. Catal., B*, 2011, **101**, 451–460.
8 P. Banković, A. Milutinović-Nikolić, Z. Mojović, N. Jović-Jovičić, M. Perović, V. Spasojević and D. Jovanović, *Microporous Mesoporous Mater.*, 2013, **165**, 247–256.
9 V. Kaloidas, C. A. Koufopanos, N. H. Gangas and N. G. Papayannakos, *Microporous Mater.*, 1995, **5**, 97–106.
10 L. A. Galeano, A. Gil and M. A. Vicente, *Appl. Catal., B*, 2010, **100**, 271–281.
11 L. A. Galeano, A. Gil and M. A. Vicente, *Appl. Catal., B*, 2011, **104**, 252–260.
12 L. A. Galeano, P. F. Bravo, C. D. Luna, M. Á. Vicente and A. Gil, *Appl. Catal., B*, 2012, **111**, 527–535.
13 G. Fetter, V. Hernandez, V. Rodrıguez, M. Valenzuela, V. Lara and P. Bosch, *Mater. Lett.*, 2003, **57**, 1220–1223.
14 N. R. Sanabria, R. Molina and S. Moreno, *Catal. Lett.*, 2009, **130**, 664–671.
15 F. Kooli, *Microporous Mesoporous Mater.*, 2013, **167**, 228–236.
16 P. Salerno and S. Mendioroz, *Appl. Clay Sci.*, 2002, **22**, 115–123.
17 L. A. Galeano, M. Á. Vicente and A. Gil, *Catal. Rev. Sci. Eng.*, 2014, **56**, 239–287.
18 H. Gao, B.-X. Zhao, J.-C. Luo, D. Wu, W. Ye, Q. Wang and X.-L. Zhang, *Microporous Mesoporous Mater.*, 2014, **196**, 208–215.
19 A. Mirzaei, Z. Chen, F. Haghighat and L. Yerushalmi, *Chemosphere*, 2017, **174**, 665–688.
20 S. Khankhasaeva, D. V. Dambueva, E. Dashinamzhilova, A. Gil, M. A. Vicente and M. N. Timofeeva, *J. Hazard. Mater.*, 2015, **293**, 21–29.
21 C. B. Molina, J. A. Zazo, J. A. Casas and J. J. Rodriguez, *Water Sci. Technol.*, 2010, **61**, 2161–2168.
22 M. Kurian and R. Babu, *J. Environ. Chem. Eng.*, 2013, **1**, 86–91.
23 S. Zhou, C. Zhang, X. Hu, Y. Wang, R. Xu, C. Xia, H. Zhang and Z. Song, *Appl. Clay Sci.*, 2014, **95**, 275–283.
24 E. Garrido-Ramírez, B. Theng and M. Mora, *Appl. Clay Sci.*, 2010, **47**, 182–192.
25 H. Bel Hadjltaief, P. Da Costa, P. Beaunier, M. E. Gálvez and M. Ben Zina, *Appl. Clay Sci.*, 2014, **91–92**, 46–54.
26 H. J. Muñoz, C. Blanco, A. Gil, M. Á. Vicente and L. A. Galeano, *Materials*, 2017, **10**, 1364.
27 J. Rouquerol, P. Llewellyn and K. Sing, in *Adsorption by Powders and Porous Solids: Principles, Methodology and Applications*, ed. J. Rouquerol, P. Llewellyn and K. Sing, Elsevier, Amsterdam, The Netherlands, 2nd edn, 2013, pp. 467–527.
28 A. Gil, S. Korili and M. Vicente, *Catal. Rev.*, 2008, **50**, 153–221.
29 M. Timofeeva, S. T. Khankhasaeva, Y. A. Chesalov, S. Tsybulya, V. Panchenko and E. T. Dashinamzhilova, *Appl. Catal., B*, 2009, **88**, 127–134.
30 J. Akitt and A. Farthing, *J. Chem. Soc., Dalton Trans.*, 1981, 1624–1628.
31 B. González-Rodríguez, R. Trujillano, V. Rives, M. Vicente, A. Gil and S. Korili, *Appl. Clay Sci.*, 2015, **118**, 124–130.
32 S. Bi, C. Wang, Q. Cao and C. Zhang, *Coord. Chem. Rev.*, 2004, **248**, 441–455.
33 L. Huang, H. X. Tang, D. S. Wang, S. F. Wang and Z. J. Deng, *J. Environ. Sci.*, 2006, **18**, 872–879.
34 Z. Chen, Z. Luan, J. Fan, Z. Zhang, X. Peng and B. Fan, *Colloids Surf., A*, 2007, **292**, 110–118.
35 S. Moreno, E. Gutierrez, A. Alvarez, N. Papayannakos and G. Poncelet, *Appl. Catal., A*, 1997, **165**, 103–114.
36 Z. Gong, L. Liao, G. Lv and X. Wang, *Appl. Clay Sci.*, 2016, **119**, 294–300.
37 M. De Bock, H. Nijs, P. Cool and E. Vansant, *J. Porous. Mater.*, 1999, **6**, 323–333.
38 R. Schoonheydt and H. Leeman, *Clay Miner.*, 1992, **27**, 249–252.
39 M. Thommes, K. Kaneko, A. V. Neimark, J. P. Olivier, F. Rodriguez Reinoso, J. Rouquerol and K. S. Sing, *Pure Appl. Chem.*, 2015, **87**, 1051–1069.
40 K. S. W. Sing, D. H. Everett, R. A. W. Haul, L. Moscou, R. A. Pierotti, J. Rouquerol and T. Siemieniewska, *Pure Appl. Chem.*, 1985, **57**, 603–619.
41 J. G. Carriazo, *Appl. Clay Sci.*, 2012, **67–68**, 99–105.
42 S. Wang, D. Minami and K. Kaneko, *Microporous Mesoporous Mater.*, 2015, **209**, 72–78.
43 M. Jaroniec, J. Choma and M. Kruk, *Colloids Surf., A*, 2003, **214**, 263–269.
44 J. Sterte and J. Otterstedt, in *Stud. Surf. Sci. Catal*, Elsevier, 1987, vol. 31, pp. 631–648.
45 F. Tomul, *Appl. Clay Sci.*, 2016, **120**, 121–134.
46 M. T. Pinho, H. T. Gomes, R. S. Ribeiro, J. L. Faria and A. M. Silva, *Appl. Catal., B*, 2015, **165**, 706–714.
47 M. Munoz, P. Domínguez, Z. M. de Pedro, J. A. Casas and J. J. Rodriguez, *Appl. Catal., B*, 2017, **203**, 166–173.
48 C. B. Molina, J. A. Casas, J. A. Zazo and J. J. Rodriguez, *Chem. Eng. J.*, 2006, **118**, 29–35.
49 C. di Luca, P. Massa, J. M. Grau, S. G. Marchetti, R. Fenoglio and P. Haure, *Appl. Catal., B*, 2018, **237**, 1110–1123.

 This journal is © The Royal Society of Chemistry 2018